Ultrathin millimeter-wave–absorbing film for automotive radars based on an epsilon iron oxide/carbon nanotube composite material

Asuka Namai*[,a], Marie Yoshikiyo[a], Jessica MacDougall[a], Takashi Ono[b], Takahiro Asai[b], Masayuki Hara[b], Momoe Kanai[b], Takayuki Yoshida[c], Yasuto Miyamoto[c], Kenji Sakane[c], Shinji Kurahashi[d], Toshifumi Nishio[d], and Shin-ichi Ohkoshi*[,a,e]

[a]*Department of Chemistry, School of Science, The University of Tokyo, 7-3-1 Hong, Bunkyo-ku, Tokyo 113-0033, Japan.*

[b]*Tokyo Ohka Kogyo Co., Ltd., 1590 Tabata, Samukawa-machi, Koza-gun, Kanagawa 253-0114, Japan*

[c]*Dowa Electronics Materials Co., Ltd., 1-3-1 Kaigandori, Minami-ku, Okayama 702-8506, Japan*

[d]*Ehime Institute of Industrial Technology, 487-2, Kubota-cho, Kurume, Matsuyama city, Ehime 791-1101, Japan*

[e]*CNRS International Research Laboratory DYNACOM, 7-3-1 Hongo, Bunkyo-ku, Tokyo 113-0033, Japan*

*To whom correspondence should be addressed

E-mail: asuka@chem.s.u-tokyo.ac.jp, ohkoshi@chem.s.u-tokyo.ac.jp

Contents: **Page**

§ 1. Effect of metal substitution

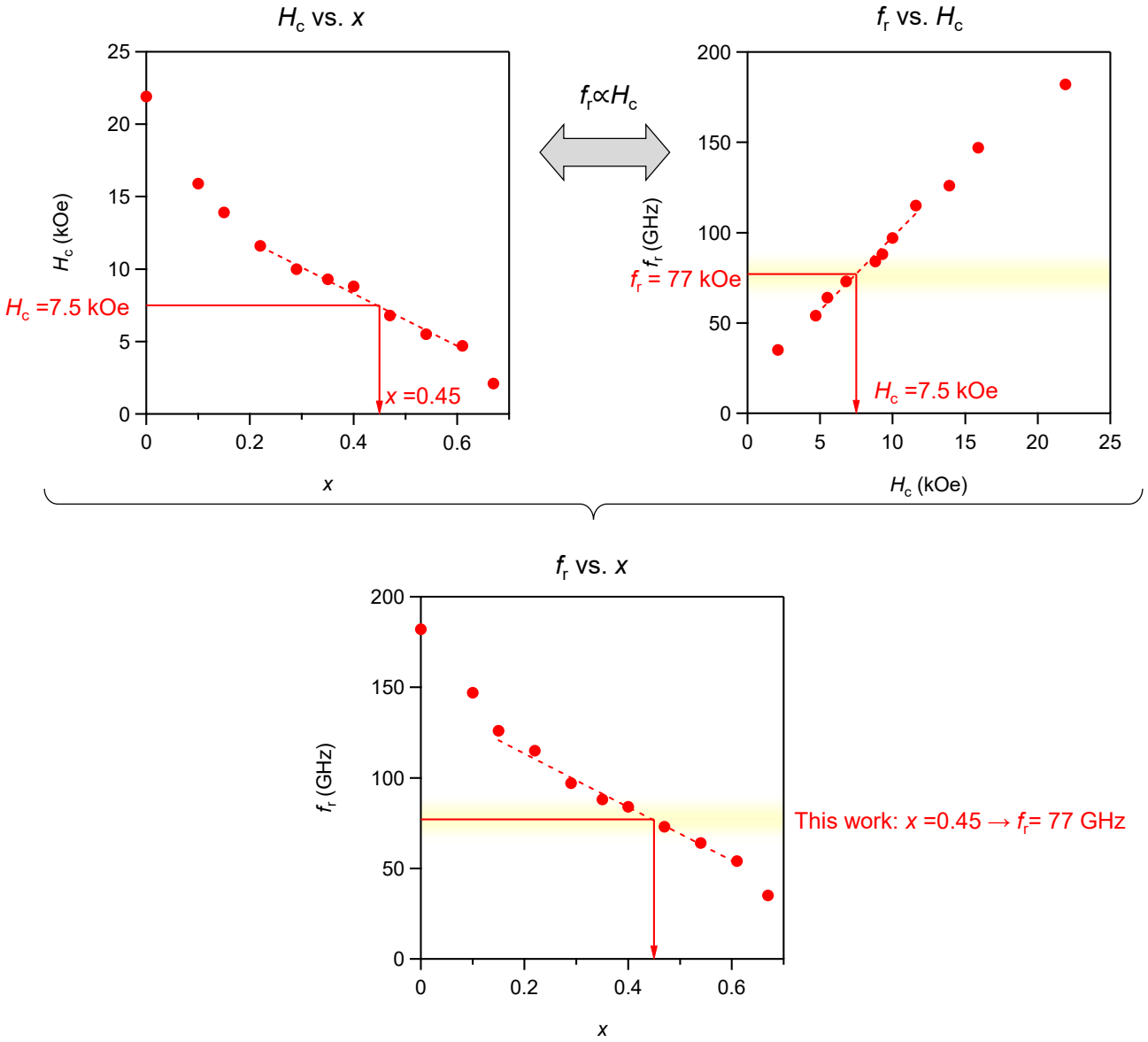

Figure S1. Relationship between the natural resonance frequency (f_r), coercive field (H_c), and substitution ratio (x) for previously reported ε-$Ga_xFe_{2-x}O_3$[26]. Based on these correlations, ε-$Ga_{0.45}Fe_{1.55}O_3$ was synthesized as a millimeter-wave magnetic absorber corresponding to the radar frequency range.

§ 2. Experimental section

Synthesis. ε-$Ga_{0.45}Fe_{1.55}O_3$ nanomagnets were synthesized by the sol–gel method according to the literature.[26] Aqueous ammonia was added dropwise to a mixed aqueous solution where $Ga(NO_3)_3 \cdot nH_2O$ and $Fe(NO_3)_3 \cdot 9H_2O$ were dissolved in water, while stirring at 30 ºC. Then $Si(OC_2H_5)_4$ was added to form a SiO_2 matrix, and the solution was stirred for 20 hours. The precipitate was collected by filtration, washed several times with water, dried at 200 ºC for 2 hours, and ground in an agate mortar. The obtained powder precursor was heated in air to 1100 ºC at a rate of 4 ºC min^{-1}, kept at 1100 ºC for 4 hours, and then cooled to room temperature at a rate of 5 ºC min^{-1}. To remove the SiO_2 matrix, an aqueous solution of NaOH was added to the sintered powder sample and stirred for 24 hours at 60 ºC. The precipitate was washed several times with water, dried, and ground in an agate mortar, yielding a brown powder.

Physical property measurements. Elemental analysis on the prepared samples was performed using inductively coupled plasma atomic emission spectroscopy (ICP-AES, Jarrel-Ash, IRIS/AP). Powder X-ray diffraction (PXRD) measurements were performed using a Rigaku Ultima IV with Cu Kα radiation (λ = 1.5418 Å). Rietveld analysis of the PXRD patterns was performed using Rigaku PDXL software. Transmission electron microscope (TEM) images were acquired with a JEOL 100CXII and JEM 2010F. The scanning electron microscope (SEM) images acquired with a JEM 7000F. The magnetic properties were measured using a superconducting quantum interference device (SQUID) magnetometer, Quantum Design, MPMS 7.

§ 3. Crystal structure analysis of ε-$Ga_{0.45}Fe_{1.55}O_3$ nanomagnets

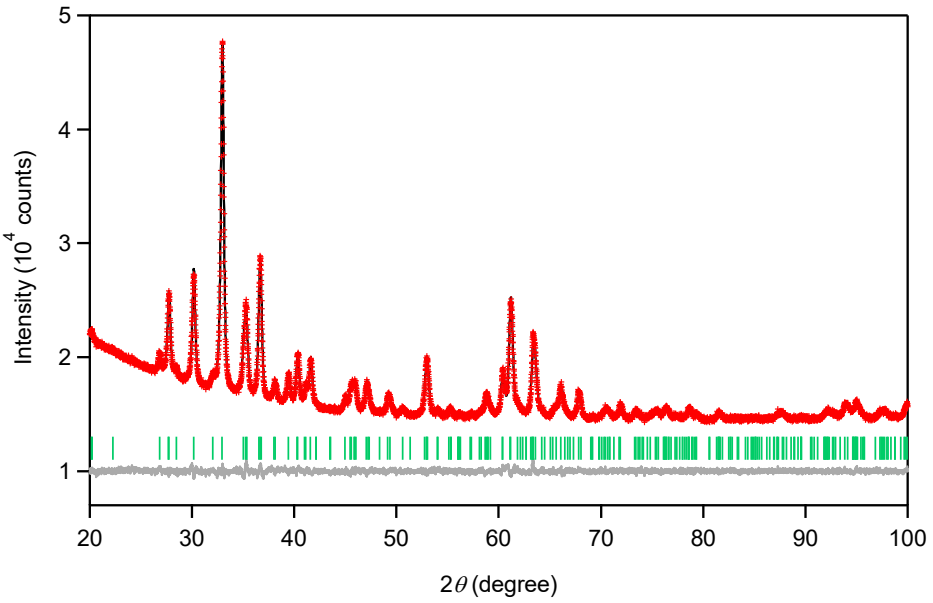

Figure S2. PXRD pattern with Rietveld analysis of ε-$Ga_{0.45}Fe_{1.55}O_3$ nanomagnets. Red dots, black line, and gray line are the observed pattern, calculated pattern, and their difference, respectively. Green bars represent the calculated positions of the Bragg reflections.

Table S1. Structural parameters of ε-$Ga_{0.45}Fe_{1.55}O_3$ obtained from Rietveld analysis of the PXRD pattern.

Polymorph		ε-$Ga_{0.45}Fe_{1.55}O_3$	
Crystal system		Orthorhombic	
Space group		*Pna*2_1 (No. 33)	
a (Å)		5.08793(10)	
b (Å)		8.7736(2)	
c (Å)		9.4375(2)	
V (Å^3)		421.289(13)	
Z		8	
R_{wp} (%)		0.88	
S		1.1561	
Ga occupancy			
Fe_A	0.01(5)		
Fe_B	0.047(13)		
Fe_C	0.375(16)		
Fe_D	0.53(2)		
Atomic pos.	*x*/*a*	*y*/*b*	*z*/*c*
Fe_A	0.317(2)	0.3502(10)	0.165(3)
Fe_B	0.3225(8)	0.0310(3)	0.368(3)
Fe_C	0.3101(6)	0.6574(5)	0.386(3)
Fe_D	0.1863(14)	0.8450(9)	0.083(3)
O1	0	0	0
O2	0.035(3)	0.323(2)	0.015(3)
O3	0.999(4)	0.653(2)	0.019(3)
O4	0.174(4)	0.4977(14)	0.271(3)
O5	0.180(4)	0.843(2)	0.267(3)
O6	0.157(3)	0.161(2)	0.242(3)

§ 4. Evaluation of μ and ε of ε-$Ga_{0.45}Fe_{1.55}O_3$ nanomagnets

The absorption spectrum measured by THz-TDS was analysed as follows. Assuming that the millimeter-wave absorption spectrum of the pellet-formed ε-$Ga_{0.45}Fe_{1.55}O_3$ sample obeys the Landau-Lifshitz equation and includes the effect from the multiple reflections within the pellet-formed sample, absorption (A) is described by the following equation.

$$A = -20\log|(\{1-[(\sqrt{\mu/\varepsilon}-1)/(\sqrt{\mu/\varepsilon}+1)]^2\}\exp(-2i\pi fd\sqrt{\mu\varepsilon}/c))/\{1-[(\sqrt{\mu/\varepsilon}-1)/(\sqrt{\mu/\varepsilon}+1)\exp(-2i\pi fd\sqrt{\mu\varepsilon}/c)]\}|, \quad (1)$$

where d, μ, and ε represent the thickness, the complex magnetic permeability ($\mu = \mu' - i\mu''$), and the complex dielectric constant ($\varepsilon = \varepsilon' - i\varepsilon''$) of the pellet-formed ε-$Ga_{0.45}Fe_{1.55}O_3$ sample, respectively, and c is the speed of light. The μ value is a function of frequency (f), which is derived from the Landau-Lifshitz equation describing the motion of the magnetization near the zero-field ferromagnetic resonance. The μ value is expressed as

$$\mu' = \mu''_{max}\sin\phi\cos\phi + 1, \quad (2)$$
$$\mu'' = \mu''_{max}\sin^2\phi, \quad (3)$$
$$\phi = \arctan[\Delta f/2(f_r - f)], \quad (4)$$

where f_r is the resonance frequency, μ''_{max} is the maximum value of μ'', and Δf is the full width at half maximum of the μ'' peak. The observed millimeter wave absorption spectrum was well-fitted with eq. (1) (Fig. S2). From the fitting, the magnetic permeability μ and dielectric constant ε of the pellet sample were obtained, calibrated with the filling ratio (Figs. 1d and S3).

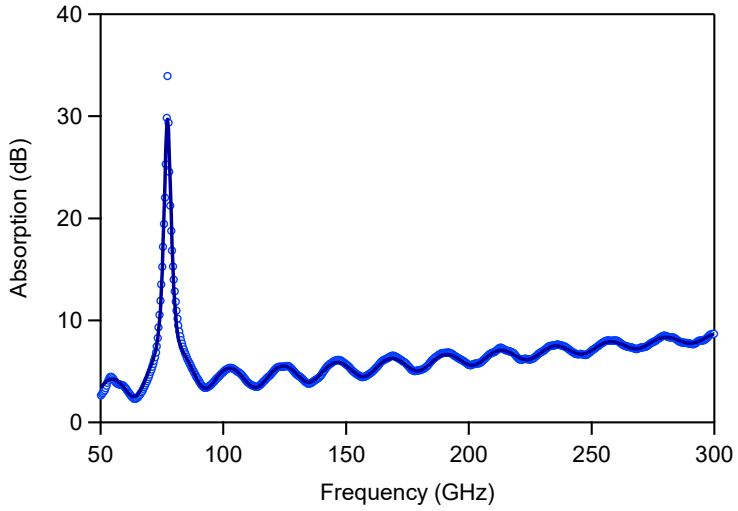

Figure S3. Absorption spectrum of the pellet-formed ε-$Ga_{0.45}Fe_{1.55}O_3$ sample. Circles and line represent the observed spectrum and the fitting, respectively.

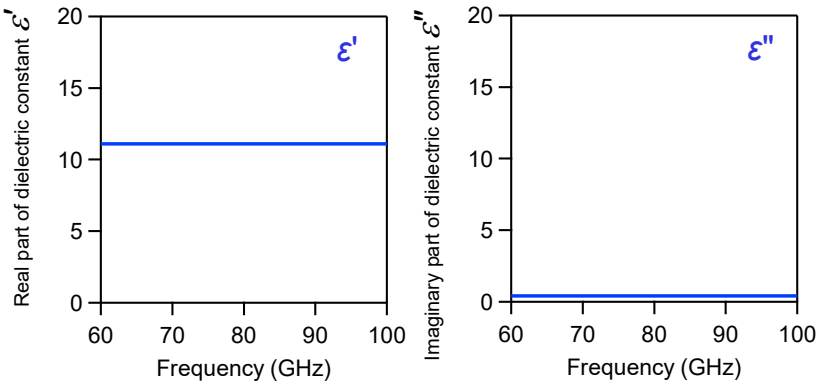

Figure S4. ε' and ε'' for ε-$Ga_{0.45}Fe_{1.55}O_3$ evaluated from the absorption spectrum.

§ 5. Morphology of CNTs

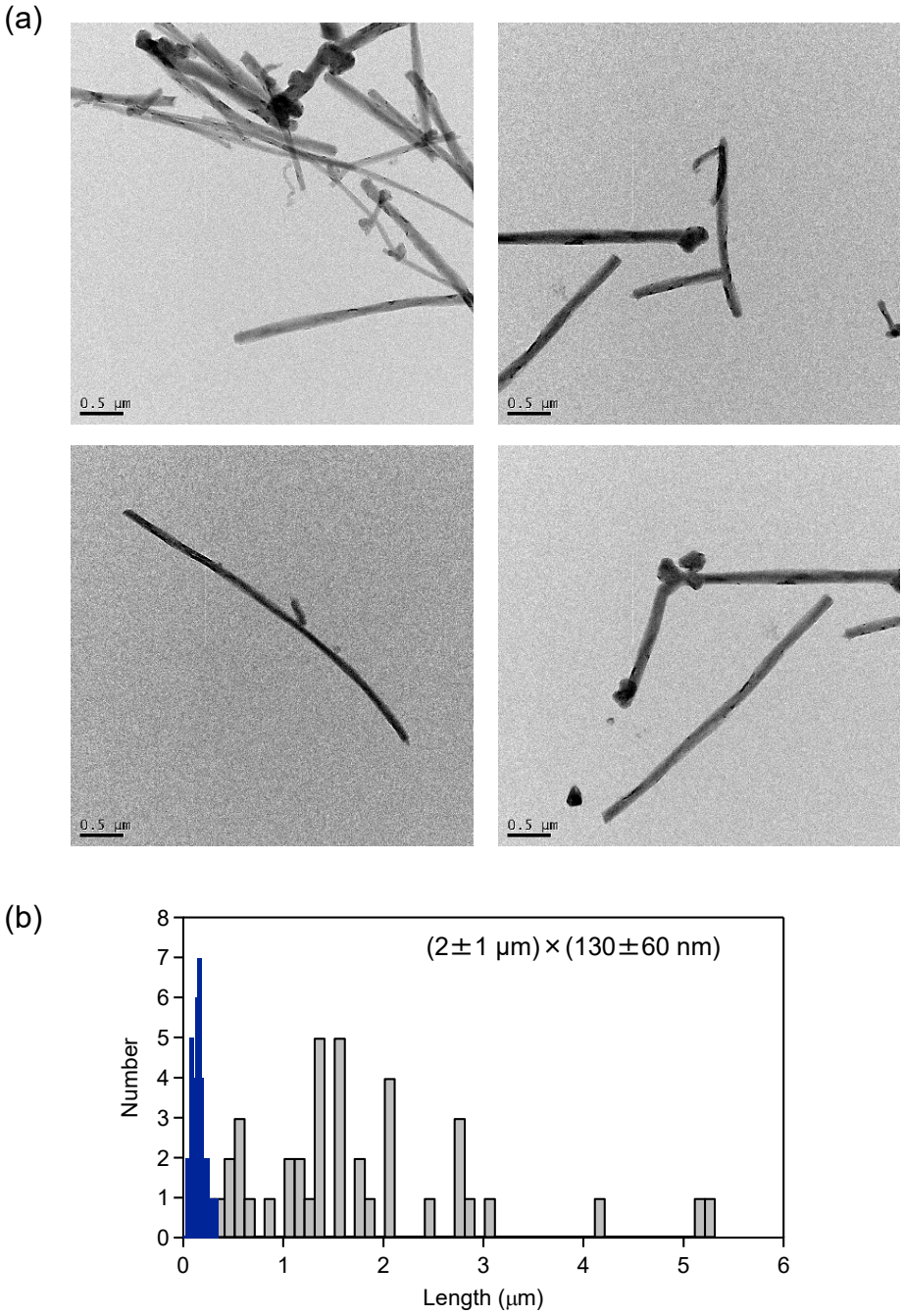

Figure S5. (a) TEM images of CNTs. (b) Size distribution of CNTs. Gray bars and blue bars represent the histograms for the long-axis and short-axis, respectively.

§ 6. Evaluation of ε of CNTs dispersed in cellulose resin

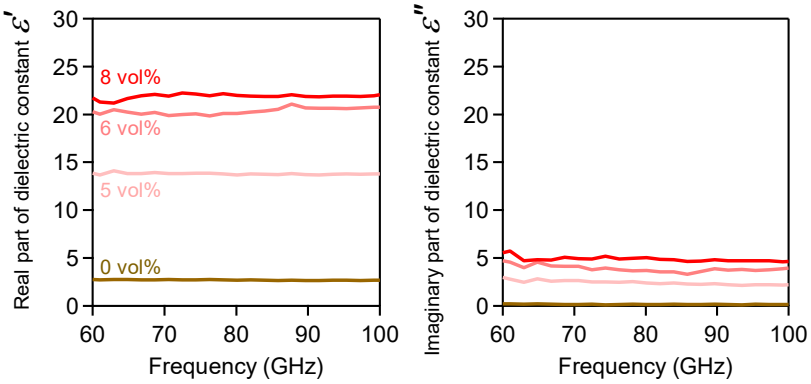

Figure S6. ε' and ε'' values for CNTs dispersed in cellulose resin with different concentrations of 0, 5, 6, and 8 vol%.

§ 7. Analysis of dielectric loss of CNTs dispersed in cellulose resin

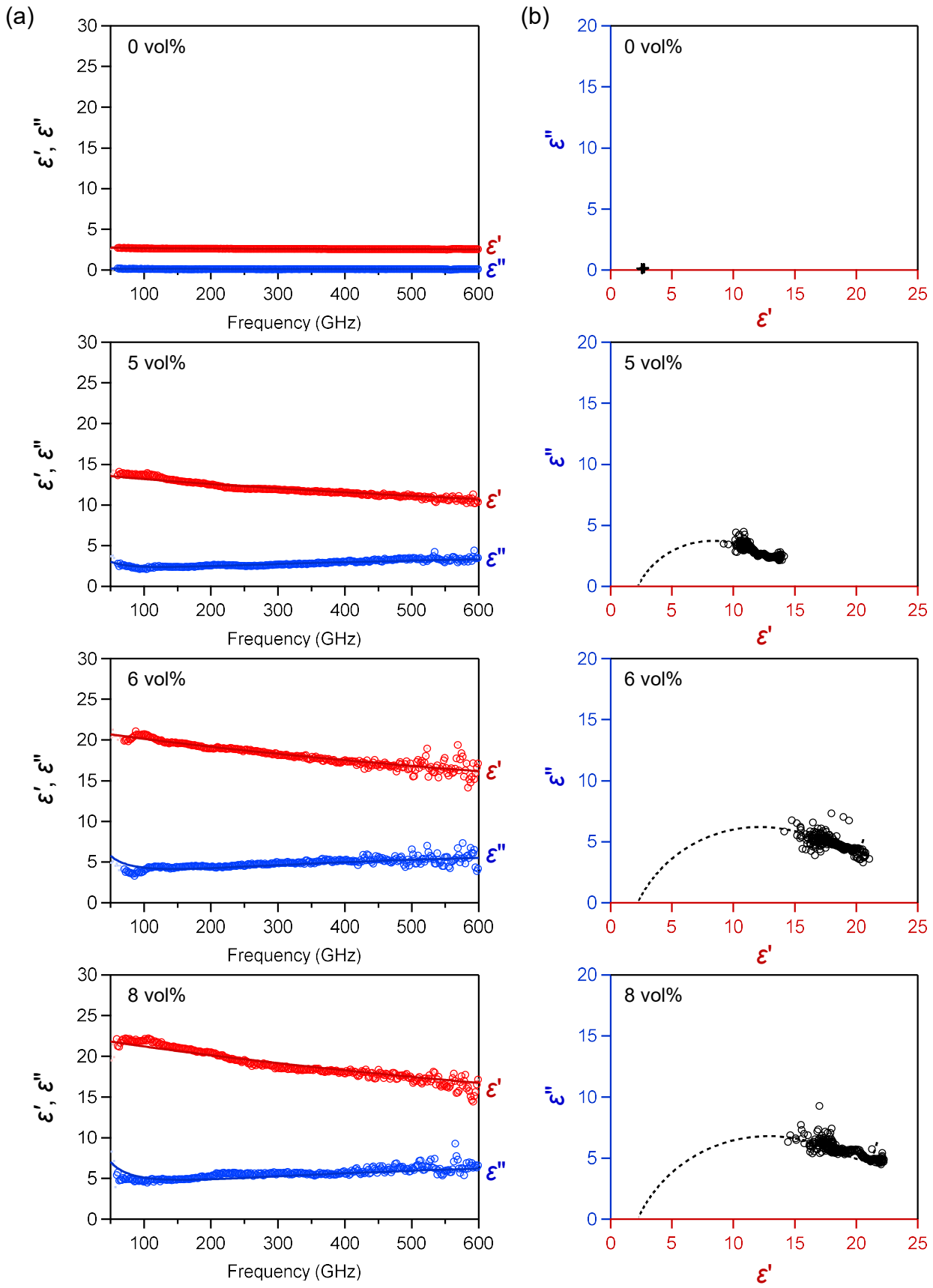

Figure S7. (a) Fitting of ε' and ε'' values using the Maxwell–Wagner–Sillars (MWS) model for CNTs dispersed in cellulose resin at different concentrations (0, 5, 6, and 8 vol%). Circles and solid lines represent experimental data and fitted curves, respectively. (b) Cole–Cole plots for CNTs dispersed in cellulose resin. Circles and dotted lines represent experimental data and fitted curves, respectively.

Table S2. The parameters in the Maxwell–Wagner–Sillars (MWS) model for CNTs dispersed in cellulose resin with different concentrations of 0, 5, 6, and 8 vol%. The value of ε_∞ refined from the 0 vol.% sample was used for all other samples, since it tends to diverge when fitted independently. Similarly, τ was fixed because its value also diverged during fitting. The other parameters were refined by simultaneous fitting of the real and imaginary parts of the dielectric constant in the frequency range of 60–600 GHz.

CNT (vol.%)	ε_∞	$\Delta\varepsilon$	τ (s)	α	σ_{dc} (S/m)
0	2.2	4.9	3×10^{-8}	0.93	0.0
5	2.2	14.5	1×10^{-13}	0.40	6.2
6	2.2	22.3	1×10^{-13}	0.35	9.4
8	2.2	23.1	1×10^{-13}	0.33	14.7

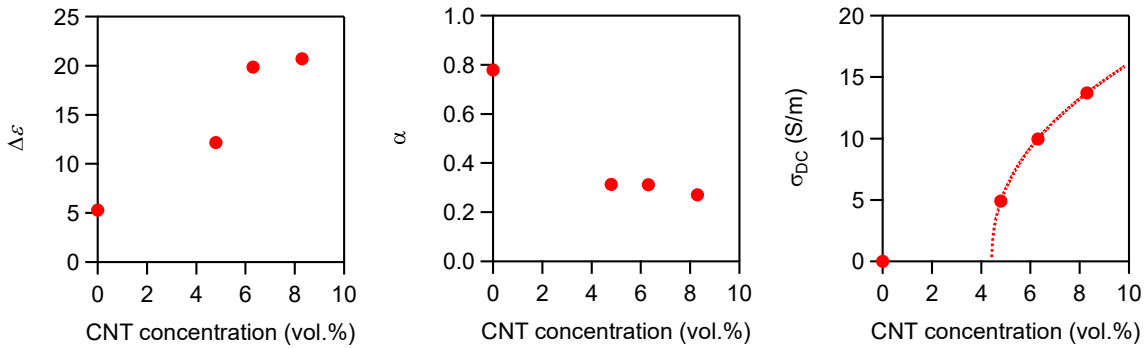

Figure S8. The plot of the refined parameters ($\Delta\varepsilon$, α, σ_{dc}) as a function of CNT concentration. In the plot of σ_{dc} versus CNT concentration, the percolation threshold was evaluated to be approximately 4.4 vol%.

§ 8. SEM of the composite

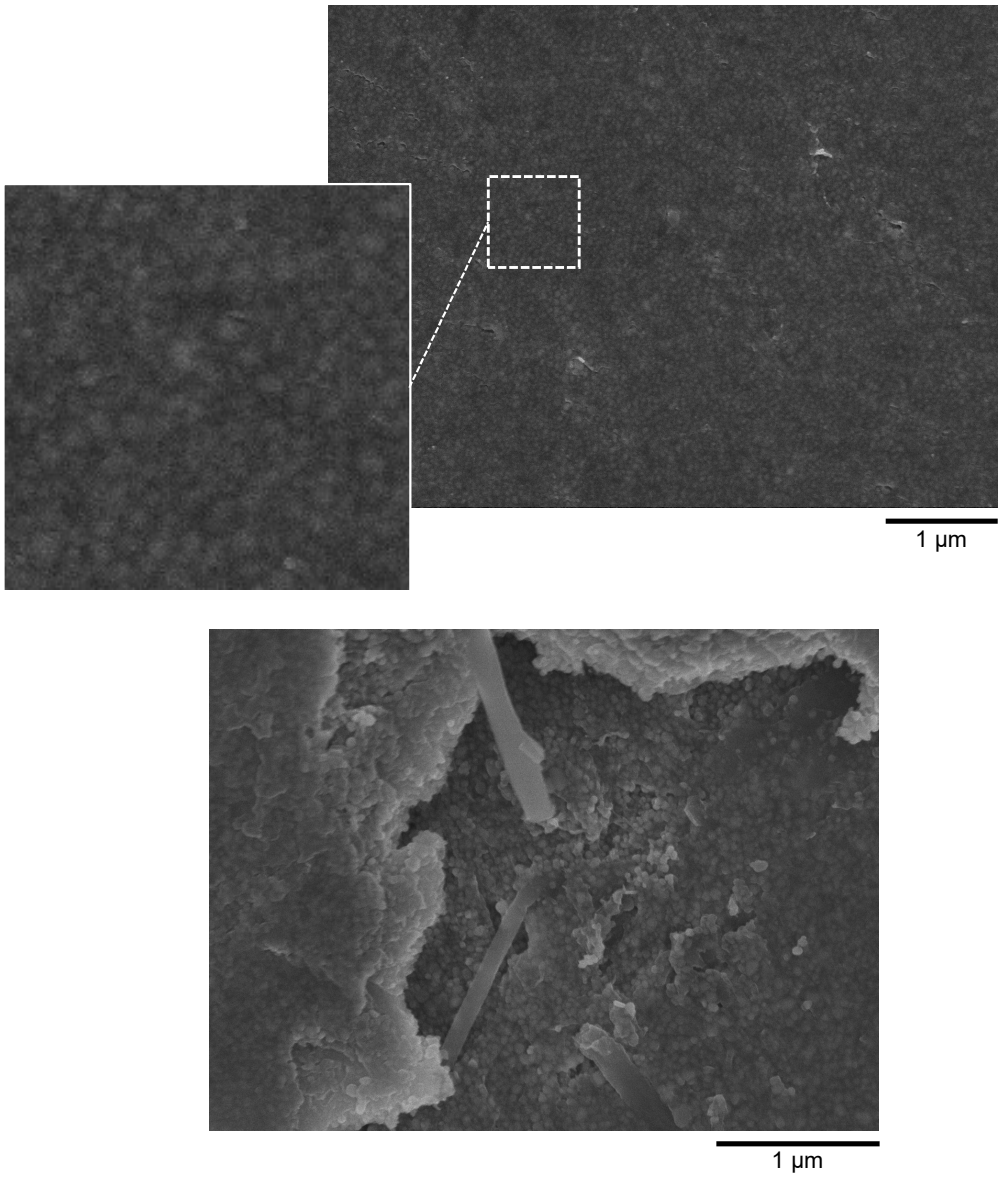

Figure S9. SEM images of the composite film. The top image shows the film surface, where ε-$Ga_{0.45}Fe_{1.55}O_3$ nanomagnets are mainly observed. The bottom image shows the interior of the film, exposed by scratching the surface, where CNTs are observed to be embedded among the ε-$Ga_{0.45}Fe_{1.55}O_3$ nanomagnets.

§ 9. Evaluation of μ and ε of the composite

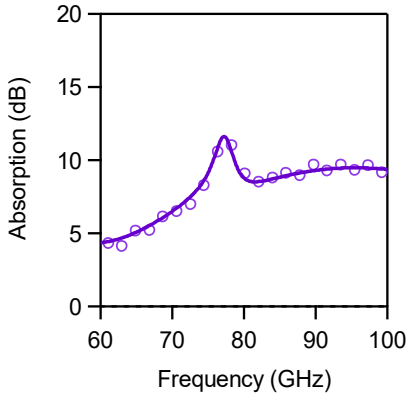

Figure S10. Absorption spectrum of the composite with 545 μm thickness. Circles and line represent the observed spectrum and the fitted line, respectively.